Eur. Phys. J. B **6**, 57–62 (1998)

THE EUROPEAN PHYSICAL JOURNAL B

Rheological behaviour and shear thickening exhibited by aqueous CTAB micellar solutions

R. Cressely[a] and V. Hartmann

Laboratoire de Physique des Liquides et des Interfaces, Groupe Rhéophysique des Colloïdes, Université de Metz,
1 boulevard F. Arago, 57078 Metz, France

Received: 3 March 1998 / Revised: 16 June 1998 / Accepted: 3 July 1998

Abstract. In this experimental work we carefully investigate the rheological behaviour and in particular the shear thickening exhibited by aqueous micellar solutions of CTAB with NaSal as added counterion. We are particularly interested in the evolution of the critical shear rate $\dot{\gamma}_C$ (at which shear thickening occurs) *versus* C_D, the surfactant concentration. We show that $\dot{\gamma}_C$, at fixed salt concentration C_S, increases with C_D following a power law evolution with a positive exponent of $+5.8$. On the other hand we show that if the ratio C_D/C_S is fixed, $\dot{\gamma}_C$ decreases with C_D with a negative exponent of -2.0. Nevertheless investigations of the zero shear viscosity η_0 indicate that in all situations (implying variation of the surfactant concentration C_D, or the salt concentration C_S or the temperature) $\dot{\gamma}_C$ is a decreasing function of the length of the micelles. All these evolutions are compatible with a gelation mechanism which could possibly be associated with entanglement effects of large interacting flowing structures.

PACS. 82.70.Dd Colloids – 83.85.Cg Rheological measurements – 83.50.Qm Thixotropy; thickening flows

1 Introduction

The rheology of aqueous cationic micellar solutions has been extensively studied over the past twenty years. If some linear properties are now well understood, a remaining intriguing problem concerns the mechanism of formation and the exact nature of shear induced structures ("SIS") corresponding to shear thickening effect. Often, at low shear rates, the diluted (or semi-diluted) surfactant solutions behave like Newtonian fluids. However, sometimes, when a critical shear rate $\dot{\gamma}_C$ is exceeded, the viscosity increases due to the formation of SIS. The magnitude of the shear thickening effect and the characteristics of this phenomenon depend on numerous factors: the nature and concentration of added salts and of the detergent, the temperature, ... It has been shown that cationic surfactants, at very small concentrations, in combination with a variety of different organic ions, *e.g.* sodium salicylate (NaSal), can be used as drag reducing agent in water. It seems that the two phenomena, shear thickening (SIS) and drag reduction are correlated. Many different techniques, such as reology, flow birefringence, neutrons scattering, conductivity, ... have been used to investigate SIS. But despite the numerous studies on the subject, a consensus on the origin and the nature of microstructures involved has not yet been achieved. Different models were presented to explain the shear induced state, as for example: an orthokinetic coagulation [1,2], a flow induced gelation by end-to-end collision [3], growth of the micelles due to thermodynamic reasons [4,5], an induced hexagonal liquid crystalline phase or nematic domains [6,7], a couplage between electrostatic and shear flow [8]. Recently using a novel light scattering visualization technique, Liu and Pine [9] have suggested that the shear thickening effect is a shear induced gelation followed by a fracture of the gel. SIS have been mostly found in cationic surfactant systems which usually include salt counterion or a cosurfactant. It was often suggested that the charge on micelles and electrostatic interactions could play an indispensable role in the occurrence of the shear induced supermolecular structures. But, for example, in a recent paper, Hu and Matthys [10] report some rheological and rheo-optical results obtained with non ionic surfactant solutions that show clear evidence of SIS formation. For such non ionic micellar systems it is obvious that electrostatic interactions is not of major importance. It is still unclear whether a universal SIS exists for different surfactant systems. It seems evident that new experimental studies, in well defined situations, in which clear shear thickening is observed, are necessary to try to understand the exact mechanism and the precise nature of shear induced state. It is the aim of this paper to give quantitative results concerning the evolution of the critical shear rate $\dot{\gamma}_C$ at which the shear thickening occurs and rheological measurements for the classical cationic surfactant cetyltrimethylammonium bromide (CTAB) in the presence of sodium salicylate (NaSal). Influence of the surfactant concentration is investigated in this work and in comparison with our

---

[a] e-mail: `cressely@lpli.sciences.univ-metz.fr`

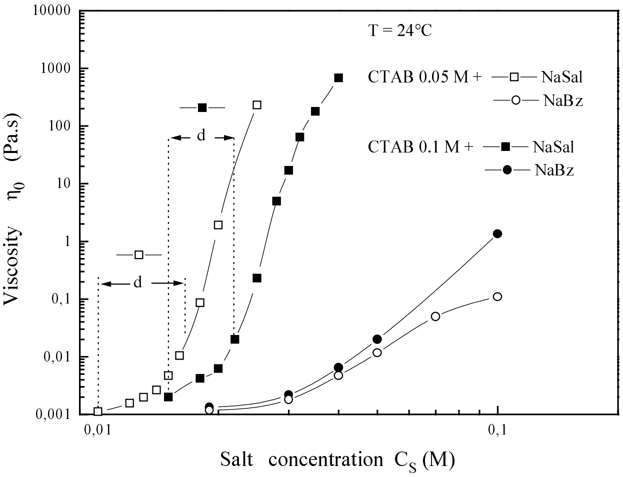

Fig. 1. Variations of the zero shear viscosity η_0 as a function of the NaSal or NaBz concentrations C_S at two surfactant concentrations $C_D = 0.05$ or 0.1 M.

previous work concerning salt influence (concentration and nature) [11–13] or temperature effect [13,14], coherent results are obtained. It should be noticed that the surfactant concentration used in this work is much greater than usually in similar studies.

2 Materials and methods

In a first step we prepared a master solution of sodium salicylate (NaSal) in distilled water, by weighing appropriate amounts of water and NaSal. The concentration (per kg) of this salt is 0.019 M. Different amounts of the surfactant CTAB (cetyltrimethylammonium bromide) were then added to this solution to obtain the desired surfactant concentrations C_D. We waited for three days in order to reach equilibrium before beginning the measurements. We have also used in this work sodium benzoate (NaBz) as added salt instead of NaSal. The structures of the two organic additives are quite similar in some aspects (a benzyl ring, ...) But, as it is shown in the following part, NaBz gives no shear thickening effect. This example shows the highly restrictive conditions necessary to obtain SIS.

The Carri-med CSL100 working in the imposed shear stress mode with a cone and plate device was used to measure all the rheological properties of the micellar solutions at equilibrium (at a temperature of 24 °C). As the critical shear rate $\dot{\gamma}_C$ should be device dependant, all the results presented in this work correspond to a unique device characterized by an angle of 0.5° and a radius of 4 cm.

Here, we have only studied the influence of the different parameters (concentrations C_S of the salt or C_D of the surfactant) in the neighbourhood of the domain giving shear thickening effect.

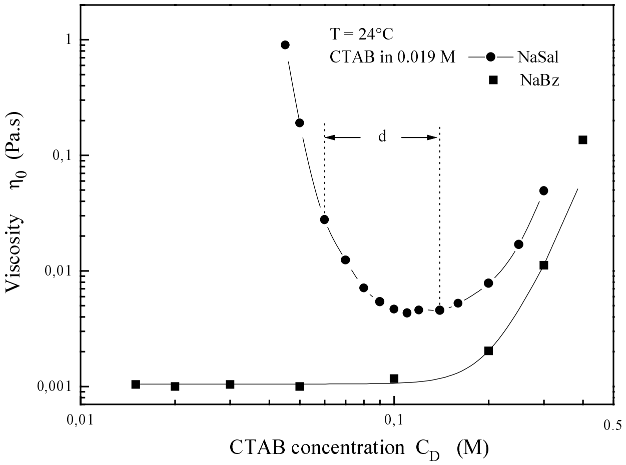

Fig. 2. Evolutions of the zero shear viscosity η_0 as a function of the CTAB concentrations C_D in 0.019 M NaSal or NaBz.

3 Results

3.1 Linear behaviour

3.1.1 Influence of the salt concentration

In Figure 1 we have represented the evolution of the zero shear viscosity η_0 against the salt concentration C_S for the two relatively similar organic salts NaSal and NaBz and for two CTAB concentrations C_D: 0.05 and 0.1 M. We have only reported the evolution of the zero shear viscosity for small salt concentrations ($C_S \leq 0.1$ M). A complete study of the salt effect, including high salt content, giving after a maximum of $\eta_0\,(C_S)$ a decreasing evolution is given elsewhere [11]. Figure 1 shows that, for NaSal, relatively small amounts of the added salt induce an very great increase of η_0, of the orders of five order of magnitude. We can see that for NaBz the effect is also important, but for higher salt concentrations (*e.g.* 0.1 M) the increasing of η_0 is of only two or three orders of magnitude. An important and apparently strange result, at first sight, in comparing the two pairs of curves is that, for NaSal, $\eta_0\,(C_S)$ is markedly more important for $C_D = 0.05$ M than for the greater surfactant concentration 0.1 M. For NaBz, more logically, $\eta_0\,(C_S)$ is more important for the greater C_D. A more complete study of the influence of C_D will be reported in the next paragraphs.

We have also represented in Figure 1 the domains d of salt concentration in which shear thickening can be observed. We can notice that they are in the beginning of the increasing part of the $\eta_0\,(C_S)$ curves. With NaBz, in the same domain of $\eta_0\,(C_S)$, no shear thickening can be obtained.

3.1.2 Influence of the surfactant concentration

The curves represented in Figure 2 correspond to the evolutions of $\eta_0\,(C_D)$, the surfactant being dissolved in a solution of $C_S = 0.019$ M. We can see in this figure that

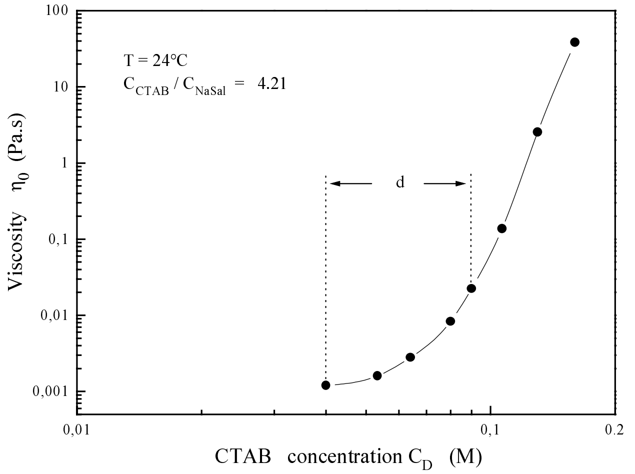

Fig. 3. Zero shear viscosity η_0 against CTAB concentration C_D at a fixed ratio $C_{CTAB}/C_{\text{NaSal}} = 4.21$.

the evolution of $\eta_0\,(C_D)$ is very different for the two salts used in this study. For NaBz the increasing of η_0 with C_D is monotonous. The increasing, after a weak evolution, becomes abrupt for $C_S > 0.2$ M. For NaSal the $\eta_0\,(C_S)$ curve, in the explored salt domain, exhibits a marked minimum. It is only near this salt concentration that it is possible to obtain shear thickening effect. The C_D domain d in which we observe this phenomenon is also represented in this figure.

In Figure 3, we have represented the evolution of $\eta_0 = f(C_D)$ at a fixed ratio $C_D/C_S = 4.21$. We can see that under this condition, η_0 is a regular increasing function of C_D. We have also indicated the domain d in which shear thickening occurs. We can notice that, like with C_S, it corresponds to the beginning of the increasing part of the $\eta_0\,(C_D)$ curve.

3.2 Non linear behaviour - Shear thickening

The curves $\eta\,(\dot\gamma)$ corresponding to NaBz are not given here. They are very classical. If they are not Newtonian for all shear rates explored, after the first Newtonian domain (corresponding to the zero shear viscosity), follows a shear thinning part, with a slow regular decreasing of the viscosity with the shear rate. Sometimes at high shear rates a phase separation occurs.

Figure 4 shows the evolution of the apparent viscosity for a selection of different CTAB concentrations solutions prepared in NaSal 0.019 M. We can notice on these curves after a Newtonian domain characterized by η_0, the occurrence of a well defined shear thickening effect, with C_D belonging to the domain d of the Figure 2. This phenomenon occurs in the concentration range corresponding to the last part of the decreasing $\eta_0\,(C_D)$ curve and in the region of the minimum exhibited by this curve. We can define $\dot\gamma_C$ as the critical shear rate corresponding to the beginning of the increase of the viscosity due to the formation of the SIS. We can see in Figure 4 that $\dot\gamma_C$ is an increasing function of the surfactant concentration C_D.

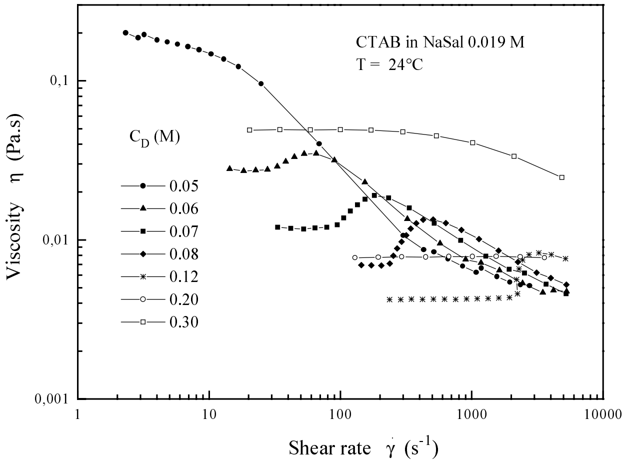

Fig. 4. Apparent viscosity η (steady measurements) as a function of shear rate for various CTAB concentrations in NaSal 0.019 M.

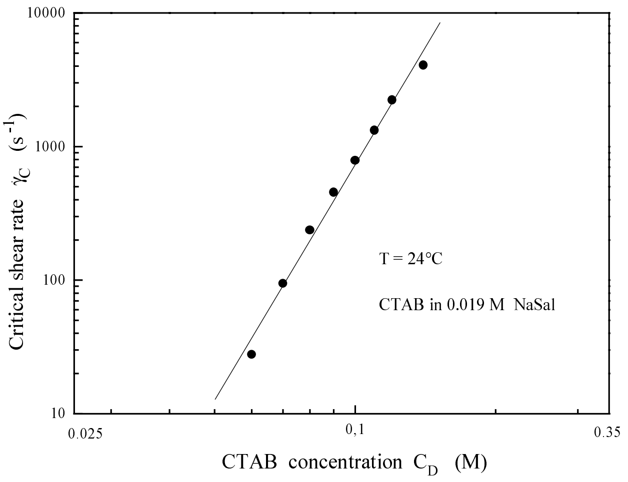

Fig. 5. Critical shear rate $\dot\gamma_C$ as a function of CTAB concentration in 0.019 M NaSal.

In Figure 5, more quantitatively we have represented, in a log-log coordinates, the $\dot\gamma_C(C_D)$ curve. The evolution is linear in this representation and characterized by a power law with a positive exponent of 5.8. At first sight this experimental result is unexpected.

To have more informations on the relative influence of surfactant and salt concentration, we have conducted rheological measurements at a constant ratio C_D/C_S (fixed here at 4.21). The results concerning the evolution of the apparent viscosity *versus* shear rate for solution giving shear thickening (or near the limit of obtaining) are given in Figure 6. We can clearly see in that figure that in these conditions, at the same temperature as before, now, $\dot\gamma_C$ is a decreasing function of the surfactant concentration C_D. More precisely, in a same log-log representation as before, the power law corresponding to the evolution of $\dot\gamma_C = f(C_D)$ is now negative, with an exponent of -2.0 (Fig. 7).

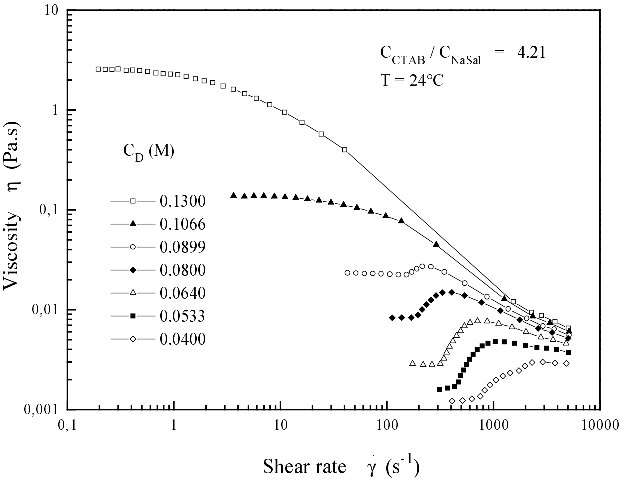

Fig. 6. Apparent viscosity (steady state measurements) plotted against shear rate for different CTAB concentrations at a fixed ratio $C_{CTAB}/C_{\mathrm{NaSal}} = 4.21$.

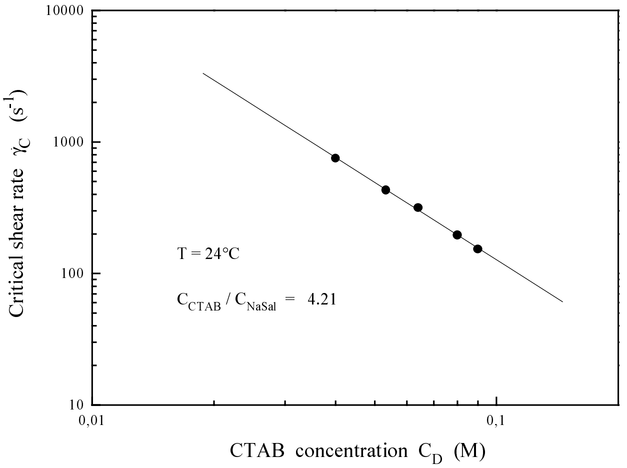

Fig. 7. Critical shear rate $\dot{\gamma}_C$ as a function of CTAB concentration at a fixed ratio $C_{CTAB}/C_{\mathrm{NaSal}} = 4.21$.

4 Discussion

4.1 Linear regime

It is known that if the CTAB concentration C_D (without NaSal) is below a critical value, an isotropic phase is obtained. Spherical micelles are present in pure aqueous solution of CTAB from the critical micellar concentration (CMC $\simeq 9.0 \times 10^{-4}$ M at 25 °C) up to approximately 0.3 M. For greater concentrations the micelles start to grow in size, giving rodlike micelles and viscoelastic solutions. At a concentration of the order of 0.6–0.7 M (depending on the temperature) a nematic phase is obtained [15]. Addition of a small amount of NaSal modifies strongly the evolution of the structure of the solution [16–18]. Proton NMR spectroscopy [19] have revealed that with $C_S < C_D$, almost all NaSal dissociate and Sal^- ions form complexes with CTA^+ to form threadlike micelles. The Sal^- ions are strongly adsorbed on the micellar surface with the carboxylic COO^- groups sticking out of the micelle [20]. The action of NaSal is very different from that of a simple salt and is in some aspects similar to that of a cosurfactant. Here in all situations where shear thickening occurs we have $C_S < C_D$. Figures 1 and 3 show that the domain d in which SIS is possible corresponds to the beginning of the growing part of the $\eta_0\,(C_S)$ or $\eta_0\,(C_D)$ (at a fixed ratio C_D/C_S) curves. This implies that the state of the solution, at rest, corresponds in these studies, to the domain where the micelles are elongated, growing in size, and beginning to significantly overlap. The increasing size of the micelles can be obtained by addition of salt (Fig. 1) or without salt by increasing the surfactant concentration. In presence of salt the evolution $\eta_0\,(C_D)$ can be more complicated as indicated for NaSal in Figure 2. In the corresponding situation, when C_D increases, it is expected, that the $\eta_0\,(C_D)$ curve must increase, as it is shown in this figure for NaBz (but with this salt no shear thickening effect can be evidenced in our experiments). An unexpected evolution of η_0, at the first sight, is often observed in the variation of $\eta_0 = f(C_S)$ for high salt content. When the high salt concentration increases, the zero shear viscosity decreases (at a fixed surfactant concentration). Evolution of this type can be observed for organic or simple mineral salt [11,21,22]. Roughly two types of explanations can be used to explain these evolutions. A simple one [23–25], relating directly the zero shear viscosity η_0 to the mean size of the micelles, suppose that at high salt concentrations, complex electrostatic interactions induce a diminution of the micellar size. A more recent hypothesis [26,27] suggests the formation of intermicellar sliding connections between the micelles (at high salt content). These sliding connections could induce a decrease of the η_0 viscosity. The decreasing part of $\eta_0\,(C_D)$ for NaSal in Figure 2 corresponds to salt concentration inferior to surfactant concentration, and so, mechanisms related to those involved in the decreasing of η_0 at high salt content ($C_S > C_D$) are inappropriate to take part in the explanation of the decreasing part of $\eta_0 = f(C_D)$. An explanation can be found in the fact that when C_D rises, the relative proportion of C_S on C_D decreases (the salt concentration is fixed here). As it can be seen in Figure 1, for NaSal, a decrease of the salt concentration in a relatively small proportion can give an important decrease of the corresponding zero shear viscosity η_0 (of several order of magnitude). So the decreasing part of the $\eta_0\,(C_D)$ curve in Figure 2 can be understood as the result of the competition of two effects: a relatively weak increase of η_0 corresponding to the increase of C_D in the concerned domain and a more important decrease of η_0 resulting from the relative diminution of C_S in comparison with C_D when C_D increases. The result of these two effects is the observed decrease of $\eta_0\,(C_D)$ represented in Figure 2. We have also shown [28] that evolutions such as those observed for NaSal in Figures 1, 2 and 3 are also obtained with, for example, NaTos (sodium tosylate) giving also shear thickening.

4.2 Non linear evolutions - Shear thickening

We have displayed, as it was shown previously [6,29,30], more than ten years ago for different cationic surfactant solutions, that for CTAB with NaSal as included salt, it is possible, in very restrictive conditions to obtained well-defined shear thickening effects. Unlike simple salts, NaSal counterions are strongly bound to the micelle when $C_S < C_D$ (situation studied here). This binding decreases the electrostatic repulsion forces between the charged heads of the surfactant molecules and so promotes formation of elongated (wormlike) micelles. In this work it can be seen that the shear induced structures can only be obtained at relatively low shear viscosity ($\eta_0 \leq 20\,\eta_{water}$), in the beginning of the increasing part of $\eta_0\,(C_S)$ and $\eta_0\,(C_D)$ (for a fixed ratio C_D/C_S). This means that the micellar concentration is near or greater (but not too much) than the overlapping concentration. There exists a limited domain of micellar size in which SIS are possible. If the micelles are too short, despite the shear flow field, creation of SIS is impossible. For too long micelles, strong interactions between the micelles exist in the quiescent state, and the zero shear viscosity is relatively high and so no shear thickening behaviour can be observed. In the very diluted concentration regime, if the solution is homogeneous, there is not enough surfactant matter to permit interactions between the micelles (even in the presence of a flow field). To obtain SIS it is necessary that the micelles are sufficiently elongated. One possibility is that, under the effect of the shear flow, collision and fusion between micelles occur, resulting in the formation of a supermolecular structure (which must exhibit gel properties). This mechanism corresponds to a shear induced gelation. It is a mechanism qualitatively in agreement (but with problems of order of magnitude) with the experimental results presented here. Such a process has been suggested more than ten years ago by Hoffmann *et al.* [6,29,30]. An other possibility associated or not with the precedent could be the creation of domains of inhomogeneous micellar concentration at the critical shear rate. This shear rate could induce by entanglement effects large interacting flowing structures (large micellar aggregates more easily orientable) giving higher viscosity. At higher shear rate these aggregates can be more or less deformed, giving, in particular by orientational effects, shear thinning evolutions as observed with our solutions.

The elongated micelles under flow are subject to the Brownian motion and orientational effects of the shear flow. The relative importance of the two effects is given by the Peclet number P, defined as the dimensionless ratio of the flow rate $\dot{\gamma}$ and the rotational diffusion coefficient D_r. To permit the coalescence of the worm-like micelles and the formation of large aggregates, it is postulated that it is necessary that the particles may be oriented, so facilitating the fusion between the particles or the formation of the aggregates. It appears, as proposed by Bruinsma [2] that $P \simeq 1$ is the condition for the onset of the flow induced gelation. So, the shear induced structure is characterized by the critical velocity gradient $\dot{\gamma}_C$, its value being of the order of D_r. For very elongated particles, an approximate expression for D_r can be taken of the order of $(k_BT)/(\eta L^3)$, η being the viscosity of the suspending media and L the length of the particle. A consequence of the proposed mechanism for the shear thickening and the approximate expression of D_r is that, as observed here, the critical shear rate $\dot{\gamma}_C$ is a decreasing function of the length of the particle.

5 Conclusion

The formation of shear induce structures (SIS) is complicated and depends on the specific conditions of the surfactant system investigated. It is still unclear whether an universal shear induced structure indeed exists for the different surfactant systems. In this experimental work we have given rheological results concerning a well defined cationic surfactant system. The comparison of the evolutions of the zero shear viscosity η_0 against C_D or C_S or T [11] with the evolutions of the critical shear rate $\dot{\gamma}_C$ at which shear thickening occurs when parameters such as C_S, C_D or T are modified shows that in all cases investigated here, more the length is, easier it is possible to orientate the particle, and so to permit the creation of the shear induced structure: in all cases $\dot{\gamma}_C$ decreases with the length of the micelles. Results are in agreement with mechanisms during which large micellar structures are formed at $\dot{\gamma}_C$. In our opinion the mechanism could be related to coagulation (nevertheless with some problems) and/or a shear induced formation of separated domains of entangled micelles corresponding to inhomogenities in the flowing solution. Complementary results, with other systems and techniques seem necessary to obtain a completely satisfactory explanation of the mechanism and the exact nature of the structures involved in the shear thickening effect.

References

1. H. Hoffmann, H. Rehage, A. Rauscher, *Structure and Dynamics of Strongly Interacting Colloids and Supramolecular Aggregates in Solution*, edited by S.-H. Chen *et al.* (Kluwer Academic Publishers, Netherlands 1992), pp. 493-510.
2. R. Bruinsma, W.M. Gelbart, A. Ben-Shaul, J. Chem. Phys. **96**, 7710-7727 (1992).
3. M.S. Turner, M.E. Cates, J. Phys.-Cond. **4**, 3719-3741 (1992).
4. S.Q. Wang, J. Phys. Chem. **94**, 8381-8384 (1990).
5. S.Q. Wang, Macromol. **24**, 3004-3009 (1991).
6. H. Hoffmann, S. Hofmann, A. Rauscher, J. Kalus, Progr. Colloid Polymer Sci. **84**, 24-35 (1991).
7. S. Hofmann, A. Rauscher, H. Hoffmann, Ber. Bunsenges. Phys. Chem. **95**, 153-164 (1991).
8. V. Schmitt, F. Schosseler, F. Lequeux, Europhys. Lett. **30**, 31-36 (1995).
9. C.H. Liu, D.J. Pine, Phys. Rev. Lett. **77**, 2121-2124 (1996).
10. Y. Hu, E.F Matthys, J. Rheol. **41**, 151-166 (1997).
11. V. Hartmann, R. Cressely, Colloid Polym. Sci. **276**, 169-175 (1998).

12. V. Hartmann, R. Cressely, Europhys. Lett. **40**, 691-696 (1997).
13. V. Hartmann, R. Cressely, Coll. Surf. **121**, 151-162 (1997)
14. V. Hartmann, R. Cressely, J. Phys. II France **7**, 1087-1098 (1997).
15. G. Hertel, H. Hoffmann, Prog. Colloid Polym. Sci. **76**, 123-131 (1988).
16. Y. Sakaiguchi, T. Shikata, H. Urakami, A. Tamura, H. Hirata, J. Electron. Microsc. **36**, 168-176 (1987).
17. T. Shikata, Y. Sakaiguchi, H. Urakami, H. Hirata, J. Colloid Interf. Sci. **119**, 291-293 (1987).
18. Y. Sakaiguchi, T. Shikata, H. Urakami, A. Tamura, H. Hirata, Colloid Polym. Sci. **265**, 750-753 (1987).
19. T. Shikata, H. Hirata, T. Kotaka, Langmuir **4**, 354-359 (1988); **5**, 398-405 (1989).
20. C. Manohar, U.R.K Rao, B.S. Valauliekar, R.M. Iyer, J. Chem. Soc., Chem. Commun. 379-381 (1986).
21. H. Rehage, H. Hoffmann, Mol. Phys. **74**, 933-973 (1991).
22. S.J. Candau, A. Khatory, F. Lequeux, F. Kern, J. Phys. IV, Colloque France, C1, Suppl. J. Phys. II **3**, 197-209 (1993).
23. U. Olsson, O. Sodermann, P. Guering, J. Phys. Chem. **90**, 5223-5232 (1986).
24. R. Bachofer, R.M. Turbitt, J. Coll. Int. Sci. **135**, 325-334 (1990).
25. T. Imae, T. Kohsaka, J. Phys. Chem. **96**, 10030-10035 (1992).
26. F. Lequeux, Europhys. Lett. **19**, 675-681 (1992).
27. I.A. Kadoma, C. Ylitalo, J.W. van Egmond, Rheol. Acta **36**, 1-12 (1997).
28. V. Hartmann, R. Cressely, unpublished.
29. H. Rehage, I. Wunderlich, H. Hoffmann, Prog. Coll. Polym. Sci. **72**, 51-59 (1986).
30. I. Wunderlich, H. Hoffmann, H. Rehage, Rheol. Acta **26**, 532-542 (1987).